

Evaluation of the possibility of chaos for doubly-fed induction generator in wind power generation system

Co Nhu Van^{1,2}, Nguyen Phung Quang², Nguyen Thanh Hai¹

¹Faculty of Electrical-Electronic Engineering, University of Transport and Communications, Hanoi, Vietnam

²Institute for Control Engineering and Automation, Hanoi University of Science and Technology, Hanoi, Vietnam

Article Info

Article history:

Received Dec 14, 2022

Revised Jun 11, 2023

Accepted Jun 25, 2023

Keywords:

Bifurcation

Control chaos

Doubly fed induction generator

Lyapunov exponents

Portrait phase

ABSTRACT

The doubly-fed induction generator (DFIG) has the advantages of compactness and low cost, so it has been applied more and more in practice. However, the structure of the DFIG system is complex, multivariable, nonlinear, and difficult to control. Chaos is a phenomenon that only occurs with nonlinear dynamical systems, sensitive to initial conditions and aperiodic but it is governed by deterministic laws, unlike random perturbations. For most powertrain systems, chaos causes disadvantages, reduce performance, and even destruction of the system. By method of analysis based on theory and simulation, the paper will demonstrate the chaotic phenomenon for DFIG when the parameters of the system change into a certain value. From that set of parameters, the controller is designed to avoid or eliminate that chaotic behavior, so that the system works more reliably and with better quality.

This is an open access article under the [CC BY-SA](https://creativecommons.org/licenses/by-sa/4.0/) license.



Corresponding Author:

Nguyen Thanh Hai

Faculty of Electrical-Electronic Engineering, University of Transport and Communications

No. 3 Cau Giay Street, Ha Noi, Vietnam

Email: nguyenthanhhai@utc.edu.vn

NOMENCLATURE

R_s, R_r	: Rotor, stator resistance	$i_{sd}, i_{sq}, i_{rd}, i_{rq}$: dq components of the stator, rotor current
L_m, L_r, L_s	: Mutual, rotor, stator inductance	u_s, u_r	: Vector of stator, rotor voltage
T_r, T_s	: Rotor, stator time constant	$u_{rd}, u_{rq}, u_{sd}, u_{sq}$: dq components of the stator, rotor voltage
σ	: Total leakage factor	Ψ_s, Ψ_r	: Vector of rotor, stator flux
$\omega, \omega_r, \omega_s$: Mechanical rotor velocity, rotor and stator circuit velocity	Ψ_{sd}, Ψ_{sq}	: dq components of the stator flux
i_s, i_r	: Vector of stator, rotor current	Ψ_{rd}, Ψ_{rq}	: dq components of the rotor flux

1. INTRODUCTION

DFIG in the power generation system has the outstanding characteristics that the stator side is directly connected to the grid and the rotor side is connected to two back-to-back voltage source converters to the grid. Because the control device is located in the rotor, the power of the control device is much smaller than the generator power (in the limited speed range, the power of the converter is only 30% of the power transmitted to the grid [1], [2]), which is economically attractive, especially when the generator power is large. The system is capable of operating in a slip coefficient in a fairly wide range ($\pm 33\%$ compared with the synchronous

speed) [3], [4] allowing to make good use of the power source hybridized by the main machine, which is working in either over synchronous or sub synchronous mode. In both modes, the machine supplies active power P to the grid on the stator side, and on the rotor side, the machine draws reactive power Q from the grid in the sub synchronous mode and returns the reactive power Q to the grid in the over synchronous mode.

Due to the great benefits of DFIG, this configuration has become now very popular for variable-speed wind turbines, so there are many control methods for DFIG to perfect the system, typically studied [5]–[10]. However, in industrial practice, reliability is extremely important, therefore, it is necessary to study more deeply and widely to help the system achieve the best efficiency and quality. The parameters of DFIG can change with temperature, life, and load conditions. Due to the challenging working environment of wind farms, DFIG is vulnerable to faults like gearbox faults, power converter faults, stator winding faults, rotor winding faults and velocity sensor faults. The word [11]–[13], from which the system may fall into a state of chaotic work, which results in poor system working quality and is the reason for issues and failures.

Recently, the research investigation into the bifurcations and chaos of motor drives and permanent magnet synchronous generators has received much attention [14]–[19], enabling a better comprehension of the system's dynamical activities, which may provide some information that is helpful for actual control and design work. However, research on chaos for DFIG is only a few scattered studies, that do not cover all issues of chaos in DFIG. While DFIG is considered complex, the parameters of DFIG can vary with temperature, life, environment, load conditions, etc., so the system may fall into a chaotic behavior, which makes the system's working quality poor, which is the main cause of system failure. Thus, it is necessary to have an overview and study more fully, applying chaos to control DFIG for wind power generators will lay the foundation for new research, thereby providing appropriate control structures to complete the system.

The paper is organized as follows: i) The overview of the chaos phenomenon and the identification to control chaos will be presented in section 2; ii) Section 3 will present some mathematical models of DFIG as a basis for implementing section 4 – chaos in DFIG, to perfect the system, a controller is introduced to eliminate or avoid the phenomenon of chaos; iii) The discussion will be done in section 5; and iv) Finally, section 6 presents the conclusions the of study.

2. CHAOS AND APPLICATIONS IN CONTROL

In the real world, any system is disturbed by external noise, the oscillations of systems are always nonlinear, the linearization of oscillation processes is nothing more than a simplification of the real oscillation problem, and in computer simulations, a small perturbation appears due to numerical round-off. A little perturbation that occurs in a chaotic system accumulates exponentially over time, dramatically altering the system's behavior [20], [21]. There are many chaotic regimes in nature and in human-made devices, chaotic dynamics is one of the most general methods of the evolution of nonlinear systems. When chaos intensifies mixing and speeds up chemical reactions, it is advantageous because it creates a strong mechanism for the transfer of mass and heat. Chaos is a common undesired phenomenon that can, for instance, lead to additional mechanical fatigue of the elements of construction due to their irregular vibrations. In a chaotic regime, there is a chance that no resonant energy absorption will push the system parameters over safe limits.

Chaos brings undesired results and can be self-maintaining, affecting the quality of the system. This phenomenon only manifests in nonlinear systems, is nonperiodic, sensitive to initial conditions, and follows certain laws that are not the same as noise. It was not until the last decades of the 20th century that chaos theory began to be deeply explored for powertrain systems. Because the input and output variables of the powertrain vary from the time, most of the calculations are instantaneous, to simplify the control problem we have to accept the idealized input variable and treat the drivetrain parameter as constant. However, that turns them into noise, which causes chaos in the system for a while. With the control requirements set out in the drive array, the accuracy of response, and stable operation, the application of chaos theory about the control object to increase reliability is very feasible.

The most crucial aspect of chaos motion is that it is highly sensitive to the initial conditions of the system. That is, a very small difference in the input that is amplified will make a very large difference in the output. This is shown very clearly by the simple system of (1) of Lorenz-1963 [22] when the initial conditions are different (Figures 1).

The parameters have the values $\sigma = 24.1$, $\rho = 10$, $\beta = 8/3$, Figure 1 shows that, with very little different initial conditions, from the value [0 1.799800000000000000000002 0] to the value [0 1.7998000000000001 0], but the state of the system has changed from a steady state (Figure 1(a)) to a chaotic state (Figure 1(b)).

Basically, a chaotic system has the following properties [23]–[25]:

- Nonlinearity: Chaos only occurs in nonlinear dynamical systems or systems that exhibit a certain degree of nonlinearity.

- Determinism: chaos can be predicted by simple deterministic equations, determining the domain of parameters corresponding to the chaotic solution. That is, chaos obeys one or more deterministic equations, without an element of randomness, or probability.
- Sensitive to initial conditions: A small change in the system's initial state can result in drastically different final-state behavior. As a result, even though the behavior of the system is determined by deterministic fundamental laws, it is impossible to anticipate it over the long term.
- Aperiodicity: Chaotic orbits are aperiodic, but follow a certain law or principle. People are often interested in a special form of this family called the attractor. The orbits wander forever in an internal domain, without reaching a fixed point or a closed orbit, they are attracted to a complex geometrical body called the strange attractor, which is a chaotic phenomenon [20]. In addition to being a strange mesomorphic structure, the chaotic attractor is also dynamically strange. The orbits are attracted to the attractive, but they are unstable on that set and are sensitive to initial conditions – a characteristic of chaos motion. Once inside the strange attractor, the phase portraits are confined to it and can approach any point arbitrarily attractor to the suction set but never repeat the same at a later. The phase trajectory is not stable anywhere on the strange attractor, but overall, the attractor is very stable as shown in Figure 2.

$$\begin{cases} \frac{dx}{dt} = \sigma(y - x) \\ \frac{dy}{dt} = x(\rho - z) - y \\ \frac{dz}{dt} = xy - \beta z \end{cases} \quad (1)$$

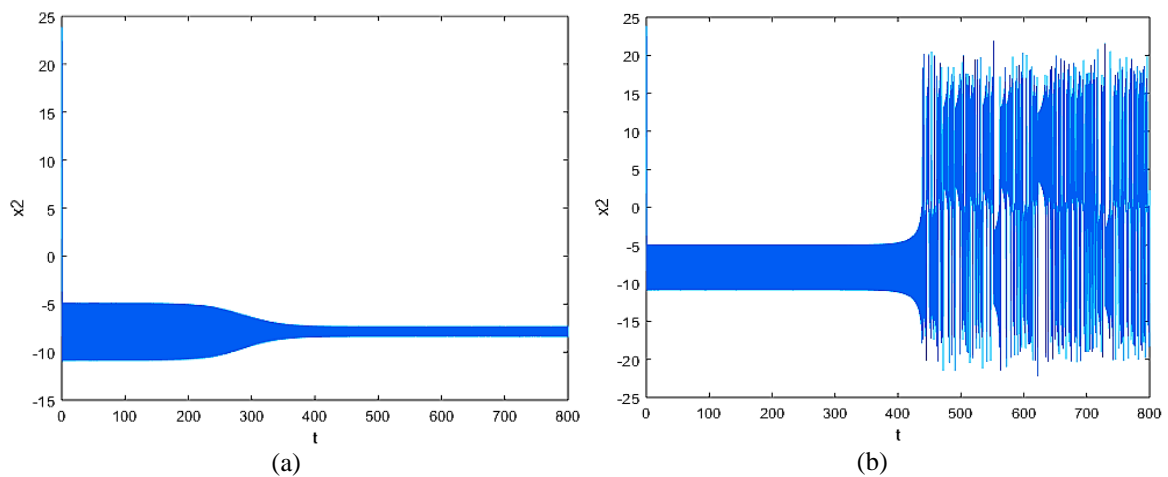


Figure 1. Simulation results of (1) for (a) system is stable and (b) the system appears to be in a chaotic state

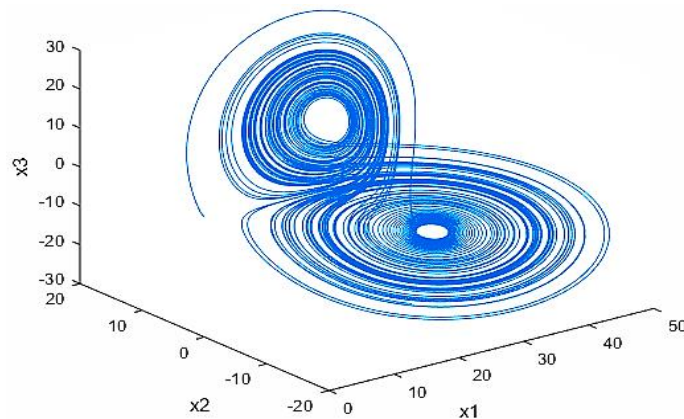


Figure 2. The attractor from the simulation of Lorenz equations on MATLAB with $\sigma = 28$, $\rho = 10$, $\beta = 8/3$

- Defining Chaos: We must first recognize that chaos never exists in a linear dynamic system. Thus, when we refer to chaos, we actually mean nonlinear systems. Chaotic motion is not present in all nonlinear systems, though. The Fourier analysis method, time responses, phase portraits, bifurcation diagrams of the maximum value of the state variable over time, and calculations of Lyapunov exponents are a few of the techniques used to identify chaos. These techniques are used to show the chaotic behavior when changing the characteristic value, to be able to identify the chaotic working area of the object, that propose controls method to eliminate the self-sustaining oscillations with high amplitude and irregular variation, return the system to a stable working state. As analyzed, the DFIG system has a complex structure, especially DFIG in wind powers working in unstable conditions from wind energy, which easily leads to a chaotic state. Therefore, identification and elimination from the "third state" in wind power generation systems using DFIG to increase reliability are important goals of this research.

3. STATE EQUATION OF DFIG

Decoupled regulation of active and reactive current components is one of the key control goals. This advises using a reference frame for the control architecture that is stator voltage orientated. The real axis of the grid voltage vector u_N might be chosen as the d axis in generating systems like wind power plants where the stator is directly connected to the grid. The following relations of the DFIM are obtained [26]:

$$\begin{cases} \psi'_{sd} = \frac{L_s}{L_m} i_{sd} + i_{rd} \approx 0 \\ \psi'_{sq} = \frac{L_s}{L_m} i_{sq} + i_{rq} \approx |\psi'_s| \end{cases} \quad (2)$$

where $\Psi'_s = \Psi_s/L_m$.

$$\begin{cases} \frac{di_{rd}}{dt} = -\frac{1}{\sigma} \left(\frac{1}{T_r} + \frac{1-\sigma}{T_s} \right) i_{rd} + \omega_r i_{rq} + \frac{1-\sigma}{\sigma} \left(\frac{1}{T_s} \Psi'_{sd} - \omega \Psi'_{sq} \right) + \frac{1}{\sigma L_r} u_{rd} - \frac{1-\sigma}{\sigma L_m} u_{sd} \\ \frac{di_{rq}}{dt} = -\frac{1}{\sigma} \left(\frac{1}{T_r} + \frac{1-\sigma}{T_s} \right) i_{rq} - \omega_r i_{rd} + \frac{1-\sigma}{\sigma} \left(\frac{1}{T_s} \Psi'_{sq} + \omega \Psi'_{sd} \right) + \frac{1}{\sigma L_r} u_{rq} - \frac{1-\sigma}{\sigma L_m} u_{sq} \\ \frac{d\Psi'_{sd}}{dt} = \frac{1}{T_s} i_{rd} - \frac{1}{T_s} \Psi'_{sd} + \omega_s \Psi'_{sq} + \frac{1}{L_m} u_{sd} \\ \frac{d\Psi'_{sq}}{dt} = \frac{1}{T_s} i_{rq} - \frac{1}{T_s} \Psi'_{sq} - \omega_s \Psi'_{sd} + \frac{1}{L_m} u_{sq} \end{cases} \quad (3)$$

Where $\sigma = 1 - L_m^2/(L_s L_r)$, $T_s = L_s/R_s$, $T_r = L_r/R_r$. In grid voltage orientated coordinates: $u_{sq} = 0$; $u_{sd} = u_s$; $\Psi'_{sd} = 0$; $\Psi'_{sq} = \Psi'_s$ and:

$$\sin \varphi = \frac{|\psi_s|/L_m - i_{rq}}{|i_s|}; m_G = -\frac{3}{2} Z_p \frac{L_m}{L_s} \psi_{sq} i_{rd} \quad (4)$$

The rotor current component i_{rd} acts as a control variable for the generator torque m_G and respectively for the active power P , because the stator flux Ψ_s is governed by the grid voltage and can be seen as constant. The power factor $\cos \varphi$ or the reactive power Q can be controlled by the control variable i_{rq} . The system of (3) shows very clearly the multivariable and nonlinear of the system, which is a necessary condition for the system to be chaotic. Thus, when the DFIG system operates under certain conditions, it can lead to chaotic behavior. This issue will be considered in detail in content 4 and content 5 below.

4. CHAOTICS PHENOMENA IN DFIG

4.1. Some causes of DFIG working unstable, bifurcation, and chaotic behavior

- When the controller parameter changes

From the classical control structure PI for DFIG in [27], based on theoretical analysis, from the Jacobian matrix, it is possible to determine the conjugate complex solutions whose real parts correspond from negative to less negative and become positive, as shown in the Table 1. One pair of complex eigenvalues' real parts become less negative as $K_{p\omega}$ increases, and at a critical value of $K_{p\omega}$, the real parts switch from negative to positive, leading to Hopf bifurcation.

- When the mechanical torque changes

The research of Yang *et al.* [28] has determined that the DFIG wind generator is capable of bifurcation to instability when the mechanical torque T_m increases to characteristic values through simulation and theoretical analysis. On the basis of theoretical analysis, the loci of the Jacobian's eigenvalues are computed and the analysis shows that the system loses stability via a Hopf bifurcation, there exist four pairs of complex

conjugating eigenvalues as T_m is varied. From Table 2 we see, for a small T_m value, all four pairs have a negative real part; as T_m increased, the real part of the eigenvalues pairs became less negative and at the critical value of T_m the real part changes from negative to 0; As T_m continued to increase, the real part became positive and the system became unstable. This suggests that the instability is caused by Hopf bifurcation.

– When DFIG is connected to a “weak” grid with unbalanced loads and parasitic

At low wind speeds, bifurcation has been identified in the DFIG wind turbine, which manifests as a low-frequency oscillation of the DC link capacitor voltage of the system when the DFIG wind turbine is coupled to a "weak" grid that has parasitic and unbalanced loads, and if the wind speed further increases, chaotic behavior may emerge [29].

– When the parameters of DFIG vary

This is a common phenomenon for DFIG during operation, and there have been studies demonstrating that chaos occurs when the parameters change to a certain value [30]–[32]. In [31], from system (5).

$$\begin{cases} \frac{d\tilde{i}_d}{d\tilde{t}} = -\tilde{i}_d + \tilde{\omega}\tilde{i}_q \\ \frac{d\tilde{i}_q}{d\tilde{t}} = -\tilde{i}_q + \tilde{\omega}\tilde{i}_d + \gamma\tilde{\omega} \\ \frac{d\tilde{\omega}}{d\tilde{t}} = \sigma(\tilde{i}_q - \tilde{\omega}) \end{cases} \tag{5}$$

Where \tilde{i}_d and \tilde{i}_q are the transformed direct-axis and quadrature axis stator current respectively; \tilde{u}_d, \tilde{u}_q are the transformed direct-axis and the quadrature-axis stator voltage components respectively; $\tilde{\omega}$ is the transformed angle speed of the motor; σ and γ are system parameters. In the case of $\tilde{u}_d(0) = \tilde{u}_q(0) = \tilde{T}_L(0) = 0$; $\sigma = 5.46$; $\gamma = 20$; $(\tilde{i}_d, \tilde{i}_q, \tilde{\omega})^T = (0.01, 0.01, 0.01)^T$ the system is chaotic.

Table 1. The eigenvalues for increasing value of $K_{p\omega}$ ($T_{L\omega} = 0:00076$) [27]

$K_{p\omega}$	Eigenvalues	Comment
128	$-1.0626 \pm j292.65, -33.743 \pm j281.95, -10.638 \pm j25.341, -3.0069 \pm j24.433$	Stable
129	$-0.2951 \pm j292.74, -34.711 \pm j282.86, -10.638 \pm j25.341, -3.0069 \pm j24.433$	Stable
129.4	$0.00136 \pm j292.78, -35.087 \pm j283.21, -10.638 \pm j25.341, -3.0069 \pm j24.433$	Unstable
130	$0.43483 \pm j292.87, -35.641 \pm j283.72, -10.639 \pm j25.341, -3.0069 \pm j24.433$	Unstable

Table 2. Eigenvalues for increasing value of T_m [28]

T_m	Eigenvalues	Comment
-0.3	$-0.0654 \pm j0.956, -0.0492 \pm j0.875, -0.0315 \pm j0.110, -0.0115 \pm j0.0851$	Stable
-0.4	$-0.0341 \pm j0.931, -0.0785 \pm j0.902, -0.334 \pm j0.127, -0.0116 \pm j0.0851$	Stable
-0.5	$-0.0018 \pm j0.934, -0.1096 \pm j0.902, -0.0347 \pm j0.145, -0.0116 \pm j0.0851$	Stable
-0.507	$0 \pm j0.935, -0.111 \pm j0.902, -0.0348 \pm j0.153, -0.0116 \pm j0.0851$	Hopf bifurcation
-0.6	$0.022 \pm j0.938, -0.1325 \pm j0.903, -0.0355 \pm j0.250, -0.0117 \pm j0.0852$	Unstable

The most recent study on chaotic phenomena and chaos control for DFIG is found in [32] typical research work, in the normal mode, through theoretical analysis of 0-1 test the system was determined to be stable. When the winding fault occurs in the system, the resistance value decreases accordingly $R_s = R_r = 0.02 \Omega$ (in nominal mode $R_s = R_r = 1\Omega$) At the same time, when the rotor speed sensor fails $\omega_0 = 2 \omega$, now the phenomenon of chaos has appeared. A fault observer based on the DFIG model is constructed to monitor the output current and the speed of the DFIG system in order to better watch the output of DFIG. Accordingly, the new sliding mode control's design is simpler, and it allows for better observation of the control effect. However, the condition of simultaneous failure of the rotor winding, stator winding, and speed sensor is rare in practice. To clarify the phenomenon of chaos for DFIG and methods to control the chaos. The following will do through the rotor winding fault condition.

4.2. Demonstration of DFIG's chaotic phenomenon based on theoretical analysis and simulation

4.2.1. State equation of DFIG

From the equation of motion of the rotor [27].

$$\frac{d\omega}{dt} = \frac{n_p}{J} \left(T_e - T_L - \frac{D}{n_p} \omega \right) \tag{6}$$

where: $T_e = \frac{3}{2} n_p L_m (i_{sq} i_{rd} - i_{rq} i_{sd})$. The control method is based on the grid voltage orientated coordinates, we have $\Psi_{sd} = 0, \Psi_{sq} = \Psi_s$, From (2) we can rewrite in (6) as (7).

$$\frac{d\omega}{dt} = \frac{n_p}{J} \left(\frac{3 n_p L_m \Psi_s}{2 L_s} i_{rd} - \frac{D}{n_p} \omega - T_L \right) \tag{7}$$

From the first 2 equations of the system of (3), combined with (7) we get the system of equations representing the rotor current on the rotating dq coordinate and the rotor speed of DFIG as (8):

$$\begin{cases} \frac{di_{rd}}{dt} = -\frac{1}{\sigma} \left(\frac{1}{T_r} + \frac{1-\sigma}{T_s} \right) i_{rd} + (\omega_s - \omega) i_{rq} - \frac{1-\sigma}{\sigma} \omega \frac{\Psi_s}{L_m} + \frac{1}{\sigma L_r} u_{rd} - \frac{1-\sigma}{\sigma L_m} u_s \\ \frac{di_{rq}}{dt} = -\frac{1}{\sigma} \left(\frac{1}{T_r} + \frac{1-\sigma}{T_s} \right) i_{rq} - (\omega_s - \omega) i_{rd} + \frac{1-\sigma}{\sigma} \frac{1}{T_s} \frac{\Psi_s}{L_m} + \frac{1}{\sigma L_r} u_{rq} \\ \frac{d\omega}{dt} = \frac{n_p}{J} \left(\frac{3 n_p L_m \Psi_s}{2 L_s} i_{rd} - \frac{D}{n_p} \omega - T_L \right) \end{cases} \tag{8}$$

where: $\Psi_{sd} = 0$, $\Psi_{sq} = \Psi_s$, $u_{sd} = u_s = U$, $u_{sq} = 0$, $\Psi'_{sq} = \Psi_{sq}/L_m$, $\Psi'_{sd} = \Psi_{sd}/L_m$, $\omega_s = 2\pi f$. The (8) is reduced to (9):

$$\begin{cases} \dot{x}_1 = c_1 x_1 + (\omega_s - x_3) x_2 - c_2 x_3 + c_3 u_{rd} - c_4 \\ \dot{x}_2 = c_1 x_2 - (\omega_s - x_3) x_1 + c_5 + c_6 u_{rq} \\ \dot{x}_3 = c_7 x_1 - c_8 x_3 - c_9 T_L \end{cases} \tag{9}$$

where: $x_1 = i_{rd}$; $x_2 = i_{rq}$; $x_3 = \omega$; $c_1 = -\frac{1}{\sigma} \left(\frac{1}{T_r} + \frac{1-\sigma}{T_s} \right)$; $c_2 = \frac{1-\sigma}{\sigma L_m} \Psi_s$; $c_3 = \frac{1}{\sigma L_r}$; $c_4 = \frac{1-\sigma}{\sigma L_m} u_s$; $c_5 = \frac{1-\sigma}{\sigma L_m T_s} \Psi_s$; $c_6 = \frac{1}{\sigma L_r}$.

$$c_7 = \frac{n_p}{J} \frac{3 n_p L_m \Psi_s}{2 L_s} = \frac{3 n_p^2 L_m \Psi_s}{2 J L_s}; c_8 = \frac{D}{J}; c_9 = \frac{n_p}{J}$$

4.2.2. With the normal operating mode of the system

Table 3 lists the key system parameters that we employed in our simulations. Figure 3 and Figure 4 illustrate when the system is operating under normal conditions. Figure 3(a) is time series diagrams of i_{rd} , Figure 3(b) is phase trajectory diagram between i_{rd} and ω . Figure 4(a) is phase trajectory diagram i_{rd} , i_{rq} and ω , Figure 4(b) illustrate all 3 Lyapunov exponents have values are negative.

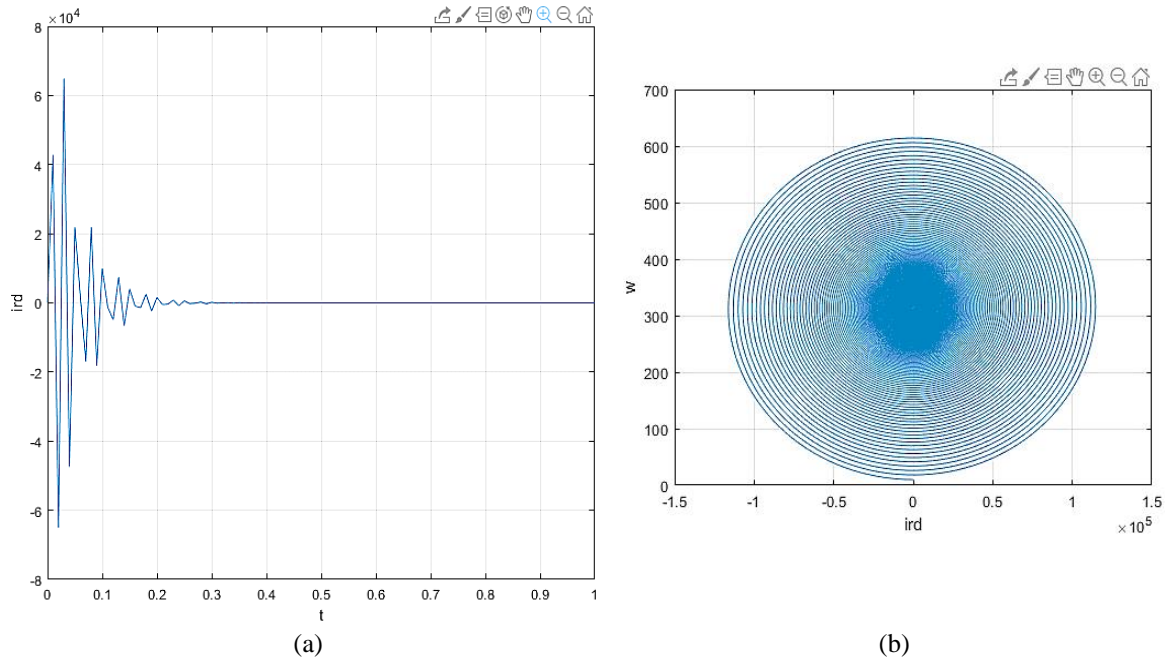


Figure 3. The system is stable under normal conditions (a) time series diagrams of i_{rd} and (b) phase trajectory diagram between i_{rd} and ω

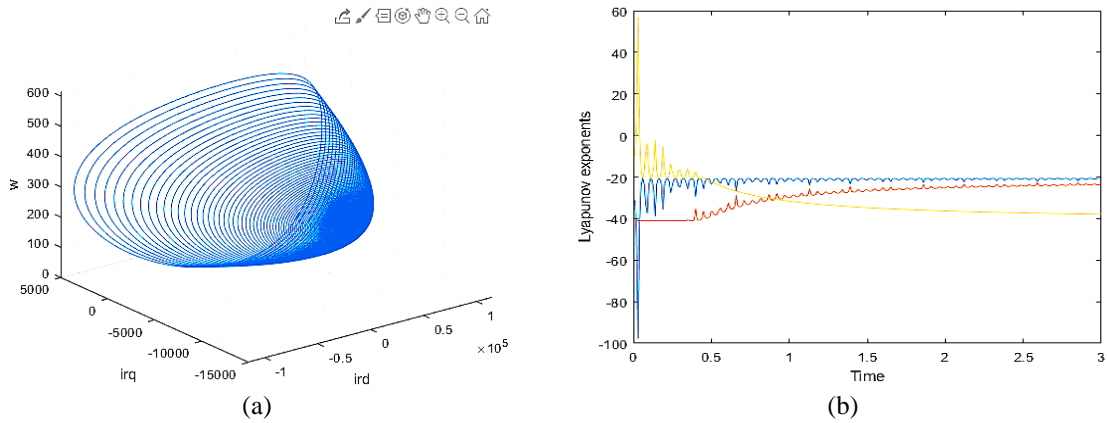


Figure 4. The system is stable under normal conditions (a) phase trajectory diagram i_{rd} , i_{rq} and ω and (b) variation of Lyapunov's exponent

Table 3. Main parameters of the DFIG system

Symbol	Parameters	Value	Symbol	Parameters	Value
U	Grid voltage (V)	575	T_L	load torque (N.m)	0
f	Grid frequency (Hz)	50	R_s, L_s	Resistance ($\mu\Omega$) and inductance (μH) of stator	20, 68
J	Moment of inertia (kgm ²)	2	R_r, L_r	Resistance ($\mu\Omega$) and inductance (μH) of rotor	21, 69
n_p	Pole pairs	3	L_m	Mutual inductance (μH)	68
D	Damping coefficient (Nm/rad/s)	0			

4.2.3. The chaotic phenomenon is determined based on theoretical analysis

In the event of a rotor winding failure, which results in the rotor resistance and inductance changing to a different value (other system parameters remain unchanged): $R_r = 15 \mu\Omega$; $L_r = 38.6 \mu H$. The equilibrium points of the system are determined by solving the system of (9), getting the following results:

$$\begin{cases} \bar{x}_1 = \frac{c_9 T_L}{c_7} \\ \bar{x}_2 = (\omega_s - \bar{x}_3) \frac{c_9 T_L}{c_1 c_7} - \frac{c_5}{c_1} \\ \frac{c_9 T_L}{c_1 c_7} \bar{x}_3^2 + \left(\frac{c_5}{c_1} - c_2 - \frac{2\omega_s c_9 T_L}{c_1 c_7} \right) \bar{x}_3 + \frac{c_9 T_L}{c_1 c_7} \omega_s^2 - \frac{\omega_s c_5}{c_1} - c_4 + \frac{c_1 c_9 T_L}{c_7} = 0 \end{cases} \quad (10)$$

Substituting the parameters in (10) and solving, we get an equilibrium point: E(0; -16310; 314,2). Stability evaluation of equilibria through Jacobian matrix: From (9) we get:

$$J_E = \begin{bmatrix} c_1 & (\omega_s - \bar{x}_3) & -c_2 - \bar{x}_2 \\ -(\omega_s - \bar{x}_3) & c_1 & \bar{x}_1 \\ c_7 & 0 & 0 \end{bmatrix}$$

$$\det[\lambda I - J_E] = \begin{bmatrix} \lambda - c_1 & -(\omega_s - \bar{x}_3) & c_2 + \bar{x}_2 \\ (\omega_s - \bar{x}_3) & \lambda - c_1 & -\bar{x}_1 \\ -c_7 & 0 & \lambda \end{bmatrix}$$

$$= \lambda^3 - 2c_1\lambda^2 + [c_1^2 + (\omega_s - \bar{x}_3)^2 + c_7(c_2 + \bar{x}_2)] \lambda - c_1 c_7 (c_2 + \bar{x}_2) - c_7 \bar{x}_1 (\omega_s - \bar{x}_3)$$

The eigenvalues of the Jacobian matrix calculated at the equilibrium point are what determine the stability of the equilibrium point. It is customary to solve equation $\det[\lambda I - J_E] = 0$ for λ .

$$\lambda^3 - 2c_1\lambda^2 + [c_1^2 + (\omega_s - \bar{x}_3)^2 + c_7(c_2 + \bar{x}_2)] \lambda - c_1 c_7 (c_2 + \bar{x}_2) - c_7 \bar{x}_1 (\omega_s - \bar{x}_3) = 0 \quad (11)$$

With the equilibrium point E(0; -16310; 314,2) the solution of (11) is determined:

$$\lambda_1 = 1,57 + j716,84; \lambda_2 = 1,57 - j716,84; \lambda_3 = -1,04$$

We see, λ_1, λ_2 are conjugate complex solutions with positive real part, so the equilibrium point E_1 is unstable. Thus, the system has 1 unstable equilibrium point. Next, we determine the Lyapunov exponent to

determine whether the system is chaotic or not. From the system of (9) with the given set of parameters, we can determine that the system has 3 Lyapunov's exponent ($\lambda_1, \lambda_2, \lambda_3$) with the same value as Table 4. We see, the system always exists at least 1 Lyapunov's exponent that is always positive, so the system has a chaotic phenomenon. For more clarity, the following simulations are performed in the following content.

4.2.4. The chaotic phenomenon is determined through simulation

From the set of parameters of the system given in section 4.2.3. The simulation results show that the rotor speed fluctuates violently and does not follow any rules as shown in Figure 5(a), component amperage i_{rd} , i_{rq} oscillates around the equilibrium point, the trajectory does not repeat the past trajectory as shown in Figure 5(b) and Figure 6(a). At the same time there is always a positive Lyapunov exponent as shown in Figure 6(b).

Table 4. Lyapunov's exponent

Time	λ_1	λ_2	λ_3	Time	λ_1	λ_2	λ_3
0.1	-6.624482	4.647723	4.647723	0.7	6.133618	-1.428603	-2.596103
0.2	2.705223	-17.230366	16.653823	0.8	9.357681	-1.139491	-6.118786
0.3	3.217109	-3.772286	2.672108	0.9	7.246686	-1.128662	-4.022807
0.4	2.930204	-2.546148	1.732098	1.0	9.052879	-0.836013	-6.123998
0.5	8.012185	-1.881995	-4.016063	1.1	9.919040	-0.756869	-7.072680
0.6	1.044099	-0.624790	1.691378				

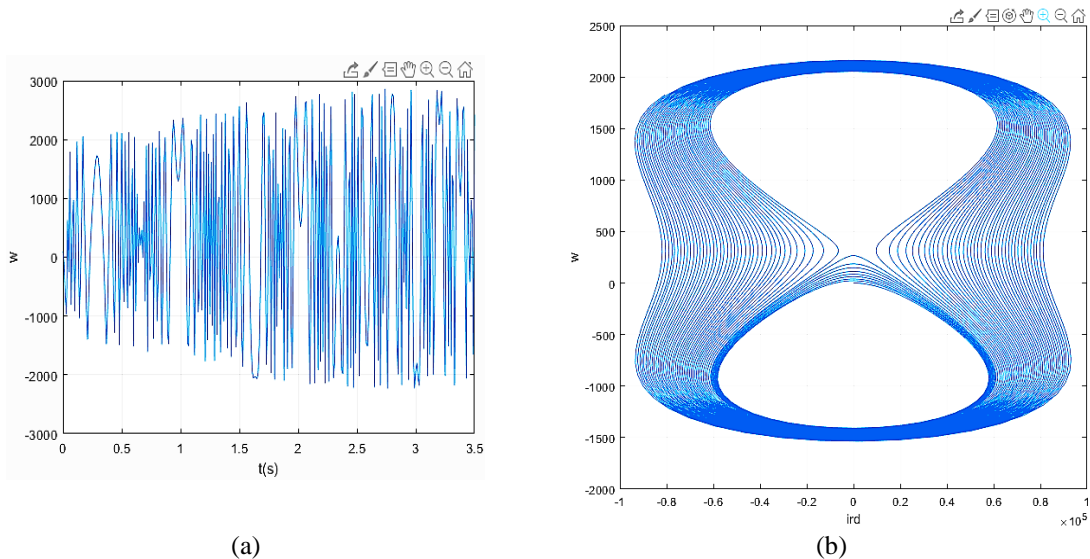


Figure 5. The system works chaotically when an error occurs (a) time series diagrams of ω and (b) phase trajectory diagram between i_{rd} and ω

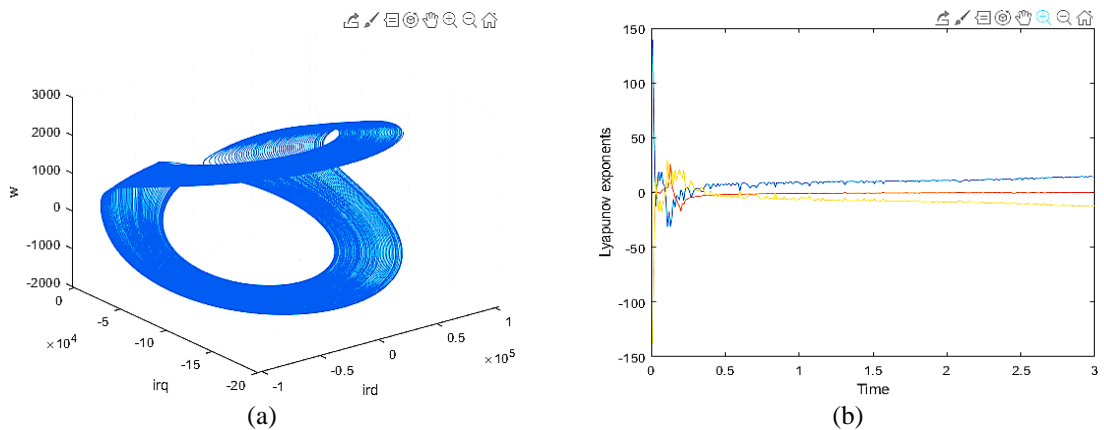


Figure 6. The system works chaotically when an error occurs (a) phase trajectory diagram between i_{rd} , i_{rq} and ω and (b) variation of Lyapunov's exponent

5. ELIMINATE CHAOTIC PHENOMENA TO STABILIZE THE SYSTEM

The chaotic phenomenon for DFIG is when the parameters of the system change to a certain value, which has been clearly shown through simulation and theoretical analysis (as shown in section 4.2). Chaos is harmful to the DFIG system, so it is necessary to design the controller to avoid or eliminate it when it occurs. The content below will take care of those issues.

When chaos occurs, the controller's task is to bring the trajectory to the equilibrium point, we use the following control law:

$$\begin{aligned}
 u_1 &= -k_1(x_1 - \bar{x}_1); u_2 = -k_2(x_2 - \bar{x}_2); u_3 = -k_3(x_3 - \bar{x}_3) \\
 \dot{x}_1 &= c_1x_1 + (\omega_s - x_3)x_2 - c_2x_3 - c_3 - k_1(x_1 - \bar{x}_1) \\
 \dot{x}_2 &= -(\omega_s - x_3)x_1 + c_1x_2 + c_4 - k_2(x_2 - \bar{x}_2) \\
 \dot{x}_3 &= c_7x_1 - c_9T_L - k_3(x_3 - \bar{x}_3)
 \end{aligned}
 \tag{12}$$

where $\bar{x}_1, \bar{x}_2, \bar{x}_3$ are equilibrium points determined from (10).

$$\begin{aligned}
 \det|\lambda I - J_E| &= \begin{vmatrix} \lambda - c_1 + k_1 & -(\omega_s - \bar{x}_3) & c_2 + \bar{x}_2 \\ (\omega_s - \bar{x}_3) & \lambda - c_1 + k_2 & -x_1 \\ -c_7 & 0 & \lambda + k_3 \end{vmatrix} \\
 &= \lambda^3 + (-2c_1 + k_1 + k_2 + k_3)\lambda^2 + [(\omega_s - \bar{x}_3)^2 + c_7(c_2 + x_2) + k_3(-2c_1 + k_1 + k_2)]\lambda + \\
 &[-c_1c_7(c_2 + \bar{x}_2) - c_7\bar{x}_1(\omega_s - \bar{x}_3) + c_7k_2(c_2 + \bar{x}_2) + k_3(\omega_s - \bar{x}_3)^2]
 \end{aligned}
 \tag{13}$$

According to the Hurwitz stability criterion, from the conditions for the system to be stable, we can choose the parameters: $k_1 = 520,000$; $k_2 = 1$; $k_3 = 1$: i) Control to eliminate the chaotic phenomenon. When chaos occurs, at 0.4 seconds the controller is inserted. Through simulation, we can see that the controller has eliminated the chaotic phenomenon, bringing the system to stable operation as shown in Figure 7(a); and ii) Control to avoid chaos: Once the boundary has been determined, the DFIG system can fall into a chaotic working state. The chaos avoidance controller will be included in the system from the very beginning. Based on the controller has been defined and the parameters have been selected. The simulation results show that the system operates stably as shown in Figure 7(b).

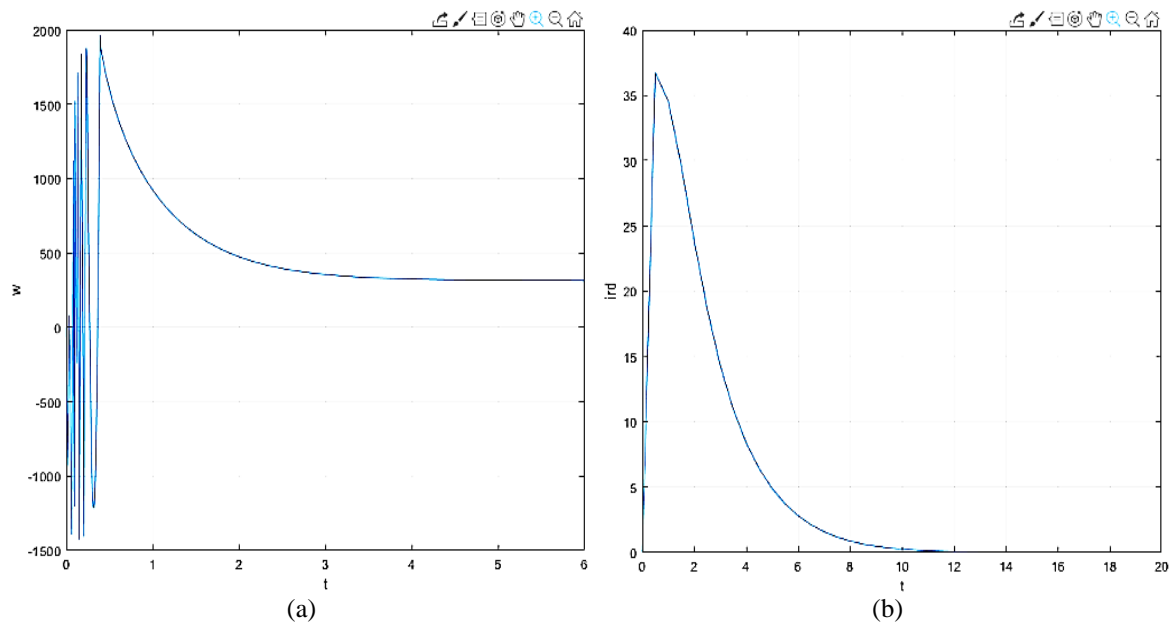


Figure 7. Simulation results when the controller is inserted for (a) time series diagrams of ω and (b) time series diagrams of i_{rd}

6. CONCLUSION

Due to DFIG's many advantages, variable-speed wind turbines are now increasingly common in this design. However, research on chaos for DFIG is only a few scattered studies, that do not cover all issues of chaos in DFIG. therefore, it is necessary to study more deeply and widely to make the system more complete.

The paper has summarized the errors that can cause DFIG to fall into the phenomenon of bifurcation and chaos, to get a general picture. At the same time, through analysis on a theoretical basis and through simulation, which has demonstrated the chaos for the system when the rotor winding fails, the working area causing chaos of the system can be determined, thereby facilitating system parameterization to build a controller to avoid or eliminate that chaos, making the system work more reliably and with better quality.

ACKNOWLEDGEMENTS

This work was supported by the Institute for Control Engineering and Automation - ICEA for their support during the research here. And this research is funded by University of Transport and Communications (UTC) under grant number T2022-DT-003.





REFERENCES

- [1] S. Müller, M. Deicke, and R. W. De Doncker, "Doubly fed induction generator systems for wind turbines," *IEEE Industry Applications Magazine*, vol. 8, no. 3, pp. 26–33, 2002, doi: 10.1109/2943.999610.
- [2] R. Pena, J. C. Clare, and G. M. Asher, "Doubly fed induction generator using back-to-back PWM converters and its application to variable-speed wind-energy generation," *IEE Proceedings: Electric Power Applications*, vol. 143, no. 3, pp. 231–241, 1996, doi: 10.1049/ip-epa:19960288.
- [3] N. P. Quang, "Review paper: General overview of control problems in wind power plants," *Journal of Computer Science and Cybernetics*, vol. 30, no. 4, Feb. 2015, doi: 10.15625/1813-9663/30/4/5762.
- [4] B. B. M. El Amine, A. Ahmed, M. B. Houari, and D. Mouloud, "Modeling, simulation and control of a doubly-fed induction generator for wind energy conversion systems," *International Journal of Power Electronics and Drive Systems (IJPEDS)*, vol. 11, no. 3, p. 1197, Sep. 2020, doi: 10.11591/ijpeds.v11.i3.pp1197-1210.
- [5] N. P. Quang, A. Dittrich, and A. Thieme, "Doubly-fed induction machine as generator: Control algorithms with decoupling of torque and power factor," *Electrical Engineering*, vol. 80, no. 5, pp. 325–335, 1997, doi: 10.1007/BF01370969.
- [6] M. Benmeziane, S. Zebirate, A. Chaker, and Z. Boudjema, "Fuzzy sliding mode control of doubly-fed induction generator driven by wind turbine," *International Journal of Power Electronics and Drive Systems*, vol. 10, no. 3, pp. 1592–1602, 2019, doi: 10.11591/ijpeds.v10.i3.pp1592-1602.
- [7] W. Yu, D. Jiang, J. Wang, R. Li, and L. Yang, "Rotor-current-based fault detection for doubly-fed induction generator using new sliding mode observer," *Transactions of the Institute of Measurement and Control*, vol. 42, no. 16, pp. 3110–3122, 2020, doi: 10.1177/0142331220941009.
- [8] T. Riouch and C. Nichita, "Advanced control strategy of dfig during symmetrical grid fault," *International Journal of Power Electronics and Drive Systems*, vol. 12, no. 3, pp. 1422–1430, 2021, doi: 10.11591/ijpeds.v12.i3.pp1422-1430.
- [9] N. Elmouhi, A. Essadki, and H. Elaimani, "Robust control of wind turbine based on doubly-fed induction generator optimized by genetic algorithm," *International Journal of Power Electronics and Drive Systems*, vol. 13, no. 2, pp. 674–688, 2022, doi: 10.11591/ijpeds.v13.i2.pp674-688.
- [10] N. Tr. Thang, *Improving the efficiency in using doubly-fed induction machine in shaft generation system on shipboards*. Nation Library of University of Transport and Communications, 2014.
- [11] S. Karimi, A. Gaillard, P. Poure, and S. Saadate, "Current sensor fault-tolerant control for WECS with DFIG," *IEEE Transactions on Industrial Electronics*, vol. 56, no. 11, pp. 4660–4670, 2009, doi: 10.1109/TIE.2009.2031193.
- [12] F. Cheng, Y. Peng, L. Qu, and W. Qiao, "Current-Based Fault Detection and Identification for Wind Turbine Drivetrain Gearboxes," *IEEE Transactions on Industry Applications*, vol. 53, no. 2, pp. 878–887, 2017, doi: 10.1109/TIA.2016.2628362.
- [13] H. Ma, T. Chen, Y. Zhang, P. Ju, and Z. Chen, "Research on the fault diagnosis method for slip ring device in doubly-fed induction generators based on vibration," *IET Renewable Power Generation*, vol. 11, no. 2, pp. 289–295, 2017, doi: 10.1049/iet-rpg.2016.0288.
- [14] Z. Q. Wu, Y. Yang, and C. H. Xu, "Fault diagnosis for permanent magnet synchronous generator under chaos conditions: LMI approach," *Wuli Xuebao/Acta Physica Sinica*, vol. 62, no. 15, 2013, doi: 10.7498/aps.62.150507.
- [15] W. Zhong-Qiang, J. Wen-Jing, Z. Li-Ru, and W. Chang-Han, "Maximum wind power tracking for PMSG chaos systems - ADHDP method," *Applied Soft Computing Journal*, vol. 36, pp. 204–209, 2015, doi: 10.1016/j.asoc.2015.07.024.
- [16] M. Messadi, A. Mellit, K. Kemih, and M. Ghanes, "Predictive control of a chaotic permanent magnet synchronous generator in a wind turbine system," *Chinese Physics B*, vol. 24, no. 1, 2015, doi: 10.1088/1674-1056/24/1/010502.
- [17] C. Wang, H. Zhang, W. Fan, and P. Ma, "Analysis of chaos in high-dimensional wind power system," *Chaos*, vol. 28, no. 1, 2018, doi: 10.1063/1.5003464.
- [18] G. A. Alamdar and S. Balochian, "Chaos control of permanent magnet synchronous generator via sliding mode controller," *Majlesi Journal of Electrical Engineering*, vol. 13, no. 1, pp. 1–5, 2019.
- [19] N. Le Hoa, L. T. Dung, and N. H. Mai, "Control of bifurcation and chaos in the model of the permanent magnet synchronous moto," *The University of Danang - Journal of Science and Technology*, vol. 1, no. 11, pp. 15–20, 2014.
- [20] N. V. Dao, T. K. Chi, and N. Dung, *Introduction to nonlinear dynamics and chaotic motion*. Vietnam National University Press, 2005.
- [21] Y. Bolotin, A. Tur, and V. Yanovsky, "Chaos: Concepts, Control and Constructive Use," p. 202, 2009.
- [22] S. H. Strogatz, "Nonlinear dynamics and chaos: With Applications to Physics, Biology, Chemistry, and Engineering," in *A Chapman & Hall Book*, 2015.
- [23] K. T. Chau and Z. Wang, "Chaos in Electric Drive Systems," Wiley, 2011.
- [24] Đ. H. N. Mi, L. T. Dung, N. P. Quang, and N. Q. Dich, "Chaotic characteristics of RFOC for three-phase AC induction motor drives," *Measurement, control, and automation*, vol. 21, no. 3, 2018.
- [25] C. N. Van, N. T. Hai, and N. P. Quang, "Wind power plants using doubly fed induction generator and the risk of chaos," 2022.
- [26] N. P. Quang and J. A. Dittrich, *Vector Control of Three-Phase AC Machines: System Development in the Practice*. Verlag Berlin Heidelberg, 2015.
- [27] L. Yang, X. Ma, and D. Dai, "Hopf bifurcation in doubly fed induction generator under vector control," *Chaos, Solitons and Fractals*, vol. 41, no. 5, pp. 2741–2749, 2009, doi: 10.1016/j.chaos.2008.10.006.





- [28] L. H. Yang, Z. Xu, J. Østergaard, Z. Y. Dong, and X. K. Ma, "Hopf bifurcation and eigenvalue sensitivity analysis of doubly fed induction generator wind turbine system," *IEEE PES General Meeting, PES 2010*, 2010, doi: 10.1109/PES.2010.5590020.
- [29] Z. Li, S. C. Wong, C. K. Tse, and G. Chu, "Bifurcation in wind energy generation systems," *International Journal of Bifurcation and Chaos*, vol. 20, no. 11, pp. 3795–3800, 2010, doi: 10.1142/S0218127410028070.
- [30] Y. Yu, Z. Q. Mi, and X. J. Liu, "Analysis of chaos in doubly fed induction generator and sliding mode control of chaos synchronization," *Wuli Xuebao/Acta Physica Sinica*, vol. 60, no. 7, 2011, doi: 10.7498/aps.60.070509.
- [31] H. Xue and Y. Wang, "Fuzzy optimal control of doubly fed induction wind power generator systems," *2010 International Conference on Mechanic Automation and Control Engineering, MACE2010*, pp. 3512–3515, 2010, doi: 10.1109/MACE.2010.5536699.
- [32] D. Jiang, W. Yu, J. Wang, G. Zhong, and Z. Zhou, "Dynamic Analysis of DFIG Fault Detection and Its Suppression Using Sliding Mode Control," *IEEE Journal of Emerging and Selected Topics in Power Electronics*, vol. 11, no. 1, pp. 643–656, Feb. 2023, doi: 10.1109/JESTPE.2020.3035205.

BIOGRAPHIES OF AUTHORS







Co Nhu Van     is a lecturer specializing in automation at the University of Transport and Communications, Hanoi, Vietnam. He received the B.E. degree in automation engineering in 2008 and the master's degree in 2013 from the University of Transport and Communications, and he is currently pursuing Ph.D. degree from Hanoi University of Science and Technology, Vietnam, both in Control and Automation Engineering. His research interests include the field of electrical drive systems, power electronics, intelligent transport systems (ITS), signal processing, and embedded system. He can be contacted at email: vancn@utc.edu.vn.



Nguyen Phung Quang     received his Dipl.-Ing. (Uni.), Dr.-Ing. and Dr.-Ing. habil. degrees from TU Dresden, Germany in 1975, 1991 and 1994 respectively. Prior to his return to Vietnam, he had worked in Germany industry for many years, contributed to create inverters REFU 402 Vectovar, RD500 (REFU Elektronik); Simovert 6SE42, Master Drive MC (Siemens). From 1996 to 1998, he served as assistant lecturer of TU Dresden where he was conferred as Privatdozent in 1997. He joined Hanoi University of Science and Technology in 1999, as lecturer up to now. He is a professor of HUST and honorary professor of TU Dresden. He was author/co-author of more than 170 journal and conference papers; 8 books with two among them was written in German and one in English entitled "Vector Control of Three-Phase AC Machines – System Development in the Practice" published by Springer in 2008, and 2nd edition in June 2015. He can be contacted at email: quang.nguyenphung@hust.edu.vn.



Nguyen Thanh Hai     is a lecturer in Faculty of Electrical - Electronic Engineering, University of Transport and Communications, Vietnam since 2002; He got the P.h.D. degree in Automation Engineering at Moscow State University of Transport Communication in 1996. He became an Associate Professor in 2013. He was with Hanoi Electronic Corporation, Vietnam as an automation engineer since 1996 to 2002. His research interests include the field of power electronic, embedded system, digital signal processing and optimal control. He has published more than 60 journal papers in the fields of automation control and power electronics. He can be contacted at email: nguyenthanhhai@utc.edu.vn.